Vol. 2 (2009) *Acta Physica Polonica B Proceedings Supplement* No 2

LHC HEAVY QUARK PERSPECTIVES*

Philippe Crochet

Laboratoire de Physique Corpusculaire, CNRS/IN2P3
Université Blaise Pascal
24, Av. des Landais, 63177 Aubière, France

(Received October 29, 2009)

After a short presentation of the motivations for measuring heavy flavors in heavy ion collisions at the LHC, the three LHC experiments ALICE, CMS and ATLAS are detailed. Then some selected physics channels are discussed.

PACS numbers: 25.75.–q, 12.38.Mh, 25.75.Nq

1. Introduction

The LHC (Large Hadron Collider) is designed to collide protons at a center of mass (c.m.) energy $\sqrt{s} = 14\,\text{TeV}$ and lead nuclei at $\sqrt{s_{NN}} = 5.5\,\text{TeV}$. This energy, which is nearly 30 times larger than the c.m. energy for Au–Au collisions at RHIC, will provide the biggest step in the history of heavy ion collisions and will open a new era for studying the properties of strongly interacting matter under extreme thermodynamical conditions. This (so far) unexplored regime is characterized by a large energy density and a close-to-vanishing baryonic chemical potential. Moreover, heavy-ion collisions at LHC access unprecedented small Bjorken-x values where low-momentum gluons are expected to be close to saturation and lead to a significant shadowing effect. Another exciting aspect of this new energy regime is the massive production of heavy quarks which allows to investigate the mechanisms of both heavy quark production and propagation in the hot and dense medium. Indeed, the production time scale of heavy quarks is shorter than that of the deconfined medium whereas their lifetime is expected to be larger than the lifetime of the medium. Therefore, heavy quarks experience the full collision history and are sensitive probes of the medium properties. This is illustrated by the recent observation at RHIC of a large suppression of high transverse

* Presented at the International Meeting "Excited QCD", Zakopane, Poland, February 8–14, 2009.

momentum (p_{t}) electrons from heavy flavor decays which is attributed to partonic energy loss of heavy quarks. At the LHC the production rate of heavy quarks is expected to exceed that of RHIC by a factor 10 for charm and by a factor 100 for bottom. Thus heavy quarks at the LHC will provide an ideal high statistics tool for a detailed characterization of the deconfined medium.

2. Heavy flavors at the LHC

The heavy flavor sector at the LHC is subject to significant differences with respect to RHIC energies. Some of these aspects are discussed hereafter. For more details, see [1]. As stated above, the charm and bottom production cross-sections are significantly enhanced at the LHC. Next-to-leading order pQCD predictions for heavy flavor production in pp collisions at $\sqrt{s} = 14\,\mathrm{TeV}$ vary within a factor 2 depending on the choice of the quark mass, the QCD renormalization and factorisation scales as well as the PDFs [2]. In Pb–Pb collisions, the charm thermal production is expected to reach $\sim 25\%$ of the charm initial production, although assuming a rather high medium temperature of 700 MeV [1]. It is interesting to observe that the uncertainty in the ratio of heavy quark cross-section at 14 TeV to that at 5.5 TeV is "only" of about 10% [3]. Therefore, a high precision measurement of heavy quark cross-section in pp collisions at $\sqrt{s} = 14$ TeV is essential. The experimental precision on this measurement is presented in the following. In nucleus–nucleus collisions, the uncertainty in the production cross-section is expected to be further enhanced due to the large uncertainty in the shadowing effect [4]. The large production rate of heavy flavors allows to use new observables for studying heavy quark quenching. The ratio of heavy to light nuclear modification factor for charm and bottom mesons is particularly interesting. It allows to probe the color charge and the mass dependence of the heavy quark energy loss, respectively. Furthermore, the ratio of bottom to charm nuclear modification factor allows to isolate the mass dependence of the energy loss and its sensitivity to the medium density is reduced [1]. Another new observable is provided by the large statistics in the single lepton p_{t} distribution. As shown in Fig. 1, the full p_{t} spectrum will be available at the LHC from very low p_{t} up to $p_{\mathrm{t}} \sim 80\,\mathrm{GeV}/c$. This allows to use the $W^{\pm}$ signal as a reference for heavy quark energy loss.

Simulations indicate that, in central Pb–Pb collisions at the LHC, heavy quark energy loss should result in a lower crossing-point of muons from heavy quarks with respect to muons from $W^{\pm}$ by 5 to $7\,\mathrm{GeV}/c$ and should suppress the muon yield by a factor 2 to 5 in the 2–$20\,\mathrm{GeV}/c$ p_{t} range [1]. Oppositely, the high p_{t} range 20–$80\,\mathrm{GeV}/c$ where muons from $W^{\pm}$ dominate is only affected by a relatively weak $W^{\pm}$ shadowing [1].

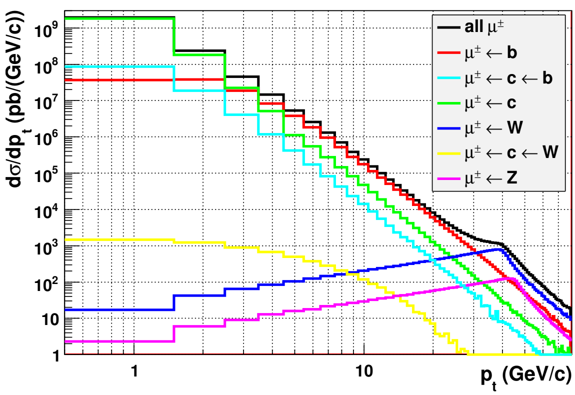

Fig. 1. Transverse momentum differential production cross-section of single muons in pp collisions at $\sqrt{s} = 14\,\text{TeV}$ [5].

3. Heavy-ion collisions at the LHC

The LHC will be operated seven months per year in pp mode and one month per year in heavy-ion mode. The corresponding estimated effective running time is 10^7 s and 10^6 s for pp collisions and heavy-ion collisions, respectively. The expected luminosity for Pb–Pb collisions is $5 \times 10^{26}\ \text{cm}^{-2}\text{s}^{-1}$ which results in a minimum-bias interaction rate of 4 kHz. As described in [6], the heavy- (and light-) ion runs include, over the first five years of operation, one Pb–Pb run at low luminosity, two Pb–Pb runs at nominal luminosity, one p–A run and one light ion–ion run. In the following years different options are considered depending on the first results.

3.1. The ALICE experiment

ALICE (A Large Ion Collider Experiment) is the only LHC experiment dedicated to the study of nucleus–nucleus collisions [3, 6]. The ALICE experiment is designed to ensure high precision measurements of numerous observables based on hadrons, leptons and photons, in a broad acceptance.

The detector consists of a central barrel, a muon spectrometer and forward/backward small acceptance detectors. The central barrel of ALICE consists of four layers of detectors placed in the solenoidal field ($B \leq 0.5\,\text{T}$) provided by the LEP L3 magnet. From the inner side to the outer side, these detectors are *(i)* the Inner Tracker System (ITS), *(ii)* the Time Projection Chamber (TPC), *(iii)* the Transition Radiation Detector (TRD) and *(iv)* the Time of Flight system (TOF). They provide charged particle reconstruction and identification in the pseudo-rapidity range $|\eta| < 0.9$, with full azimuthal coverage and a broad $p_{\rm t}$ acceptance. The ALICE central barrel will later be equipped with a large acceptance ($|\eta| < 1.4$, $\Delta\Phi = 110°$) Electromagnetic Calorimeter. These large area devices are complemented by two smaller acceptance detectors: the High Momentum Particle IDentification (HMPID) and the PHOton Spectrometer (PHOS). In the forward/backward region, additional detectors (T0, V0 and FMD) allow fast characterization and selection of the events as well as charged particle measurement in the pseudo-rapidity range $-3.4 < \eta < 5.1$. Photon multiplicity will be measured in the Photon Multiplicity Detector (PMD). At large rapidities, spectator nucleons in heavy-ion collisions will be measured by Zero-Degree Calorimeters. A muon spectrometer covering the pseudo-rapidity range $-4 < \eta < -2.4$ complements the central barrel. It consists of a front absorber, a dipole magnet, ten high-granularity tracking chambers, a muon filter and four large area trigger chambers.

Heavy flavors will be measured in ALICE in the electron channel and in the hadron channel at mid-rapidities ($|\eta| < 0.9$) and in the muon channel at forward rapidities ($-4 < \eta < -2.4$).

3.2. The CMS experiment

CMS (Compact Muon Solenoid) is a general purpose detector designed to measure muons, electrons, photons and jets. Although the detector is optimized for *pp* collisions, a strong heavy ion program has been developed for several years [7]. CMS is composed, from the interaction point to the outer side, of a tracking system, an electromagnetic calorimeter, a hadronic calorimeter and muon chambers arranged in a central barrel and two end-caps. The central element of CMS is a 13 m long, 3 m diameter magnet delivering a $B = 4$ T solenoidal field which surrounds the tracking and calorimetric systems. The tracker covers the pseudo-rapidity region $|\eta| < 2.5$. The electromagnetic calorimeter covers the pseudo-rapidity region $|\eta| < 1.5$ in the central barrel. This coverage is extended to $|\eta| < 3$ with the end-caps. The hadronic calorimeter has an acceptance covering $|\eta| < 2$ in the central barrel and reaches $|\eta| < 5.3$ with the end-caps. Two additional very-forward calorimeters ensure coverage in the pseudo-rapidity range $\pm 3 < \eta < \pm 5$. The muon system is located outside the central magnet. It consists of four layers of detectors (three for tracking and one for trigger) covering the pseudo-rapidity range $|\eta| < 2.4$ ($|\eta| < 1.5$ in the barrel). Very forward calorimeters, including two Zero Degree Calorimeters ($\pm 3 < \eta < \pm 5.2$) and a quartz fiber calorimeter ($\pm 5.3 < \eta < \pm 6.7$) allow measurements of the collision centrality and electromagnetic energy.

For the time being, the performances of CMS for heavy flavor detection in heavy ion collisions have been investigated in the muon channel only.

3.3. The ATLAS experiment

Like CMS, ATLAS (A Toroidal LHC ApparatuS) is designed for pp physics. The detector capabilities for heavy ion physics have been recently investigated [8]. The design of the detector is similar to that of CMS with a tracking system, an electromagnetic calorimeter, a hadronic calorimeter and muon chambers placed in a barrel and two end-caps. The tracking system of ATLAS is composed of silicon pixel detectors, the SemiConductor Tracker (SCT) made of silicon strip detectors, and the Transition Radiation Tracker (TRT). It is placed inside a $B = 2$ T solenoidal magnet and covers the pseudo-rapidity range $|\eta| < 2.5$. The electromagnetic calorimeter covers $|\eta| < 4.9$. It is surrounded by the hadronic calorimeter in the barrel ($|\eta| < 1.7$) and in the end-caps ($\pm 1.5 < \eta < \pm 3.2$). Two additional (electromagnetic and hadronic) calorimeters cover the very forward region ($\pm 3.2 < \eta < \pm 4.9$). The muon spectrometer consists of a toroidal magnet providing a $B = 4$ T field and several muon chambers with different technologies in the barrel and in the end-caps. The acceptance of the muon spectrometer covers $|\eta| < 1.0$ in the barrel and extends to $\eta = \pm 2.5$ in the end-caps.

As for CMS only the muon channel has been investigated so far for heavy flavor detection in heavy ion collisions.

4. Selected physics channels

4.1. Secondary J/ψ from B-hadron decay

The ratio of secondary J/ψ from B-hadron decay to direct J/ψ is expected to reach 20% (in 4π) at the LHC (assuming no hot medium effects). Due to the large lifetime of B-hadrons, identification of secondary J/ψ is done from the reconstruction of the invariant mass of dileptons with displaced vertices. Such measurements are made possible thanks to the excellent performances of the LHC detector inner tracking systems. As an example, the left panel of Fig. 2 shows the expected performances of CMS [7]. A similar performance is reached by the ALICE experiment in the electron channel [3]. These secondary J/ψ can further be used to measure the B-hadron cross-section, as it is done in CDF and D0 experiments [9], to estimate shadowing in p–A collisions, and to probe the medium-induced b-quark energy loss in AA collisions. Indeed, it has been shown that b-quark quenching results in a reduced yield of secondary J/ψ and in a significantly narrowing of their η distribution [10]. The latter measurement is particularly well adapted to CMS and ATLAS detectors which have a large η coverage.

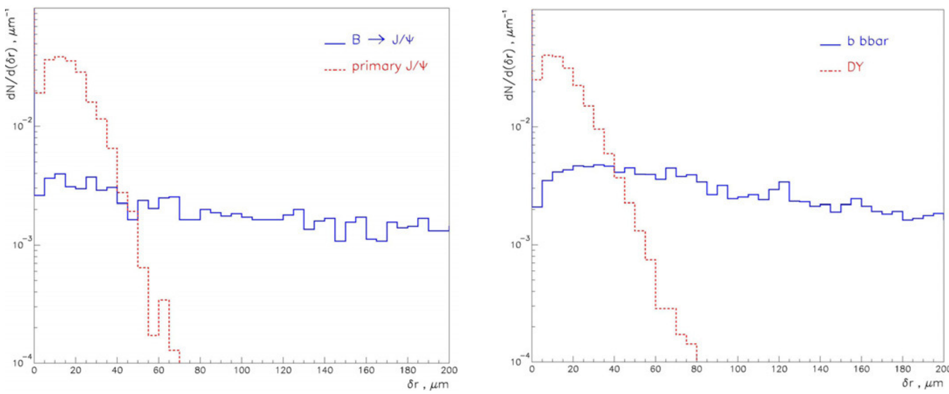

Fig. 2. Left: distance between the primary and the secondary vertices of dimuon pairs in the J/ψ mass range. The solid (dashed) histogram corresponds to secondary J/ψ from B-hadron decay (primary J/ψ). Right: transverse distance, δr, distribution for muon pairs from B-hadron decays (solid histogram) and for Drell–Yan dimuons (dashed histogram) in the high mass dimuon region. From [7].

4.2. B-hadron cross-section from dileptons

The unlike-sign dilepton mass range from 10 to 70 GeV$/c^2$ consists of dileptons from B and D hadron decays and Drell–Yan. The correlated component is dominated by dileptons from $B\bar{B}$ decay and Drell–Yan. Dileptons from $B\bar{B}$ decay appear with displaced vertices whereas Drell–Yan dileptons come from the primary vertex. Therefore, assuming that the non-correlated background can be rejected by means of appropriated techniques (*e.g.* the event-mixing technique), an analysis similar to that described in the previous section but performed in the dilepton high-mass region allows to extract the $B\bar{B}$ signal. Such an analysis has been investigated in CMS [7]. The right panel of Fig. 2 shows the distribution of δr which is defined as the distance, in the transverse plane, between two muon track distances to the primary vertex. It can be seen that the δr distribution from $B\bar{B}$ decay is rather flat whereas that of Drell–Yan is peaked at small δr values. Simulations indicate that a cut at $\delta r > 50$ μm suppresses the Drell–Yan signal by two orders of magnitude while the signal from $B\bar{B}$ is only reduced by 30% [7]. A similar analysis has been successfully performed without vertexing in the dimuon channel with the ALICE detector [3]. In this analysis, the different components in the unlike-sign dimuon spectra are unfolded using a combined fit.

4.3. B-hadron cross-section from single leptons

The B-hadron inclusive differential cross-section can be extracted from the single lepton p_t distribution using a method developed by the UA1 Collaboration [11] and further used by the CDF and the D0 collaborations at the Tevatron. The method consists of the two following steps. First, the number of leptons from bottom decay is estimated from the total lepton p_t distribution. Then, the corresponding B-hadron production cross-section is obtained in an inclusive differential way after corrections for decay kinematics, branching ratio, acceptance and efficiencies. The second step of the analysis can be achieved in a rather straightforward way by means of Monte Carlo simulations providing detection acceptance and efficiencies are known and modeled.

The first step of the analysis is achieved in a different way depending on whether or not vertexing is available. If no vertexing is available (*e.g.* ALICE-muon channel), after subtraction of the background, the different components in the lepton p_t distributions are unravelled via a combined fit which includes the shapes of the different lepton sources and their amplitude as free parameters. If vertexing is available (*e.g.* ALICE-electron channel), leptons from B-hadron decay are isolated by means of combined cuts on the lepton p_t and their distance of closest approach. Each method has its own advantages, drawbacks and specific systematics which allows for interesting cross-checks when performed simultaneously.

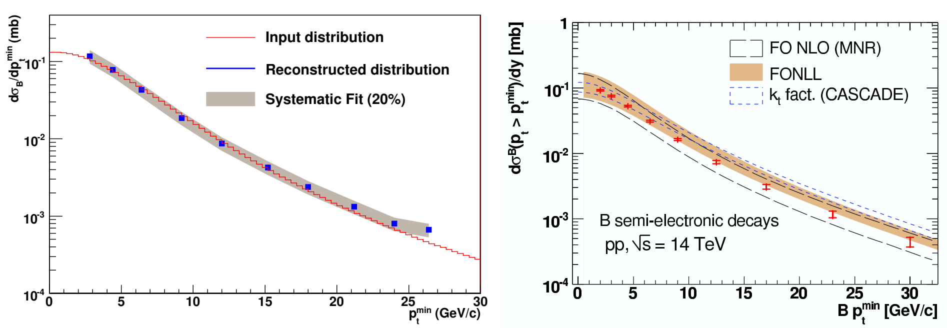

Fig. 3. Left: inclusive differential B-hadron production cross-section extracted in pp collisions (assuming $L = 10^{30}\,\text{cm}^{-2}\text{s}^{-1}$ and $t = 10^6$ s) from single muon p_t distributions in ALICE. Statistical errors are negligible. The shaded area shows systematic errors estimated to 15%. From [12]. Right: inclusive differential B-hadron production cross-section extracted from 10^9 pp minimum-bias events in the single electron channel. Statistical errors (inner bars) and quadratic sum of statistical and p_t-dependent systematic errors (outer bars) are shown. The curves correspond to the theoretical predictions from three pQCD calculations with their uncertainties. From [13].

Fig. 3 shows the reconstructed inclusive differential B-hadron production cross-section extracted in pp collisions in ALICE in the muon and the electron channels.

4.4. Hadronic charm

In the central barrel of ALICE, heavy mesons can be fully reconstructed from their charged particle decay products in the ITS, TPC and TOF [3,14]. Thus, not only their integrated yields, but also their $p_{\rm t}$ distributions can be measured. The most promising decay channel for open charm detection is the $D^0 \to K^-\pi^+$ decay (and its charge conjugate) which has a branching ratio of about 3.8 % and $c\tau = 124$ μm. The expected rates (per unit of rapidity at mid rapidity) for D^0 (and $\bar{D}^0$) mesons, decaying in a $K^{\mp}\pi^{\pm}$ pair, in central (5 %) Pb–Pb at $\sqrt{s} = 5.5\,$TeV and in pp collisions at $\sqrt{s} = 14\,$TeV are 5.3×10^{-1} and 7.5×10^{-4} per event, respectively. The selection of this decay channel allows the direct identification of the D^0 particles by computing the invariant mass of fully-reconstructed topologies originating from displaced secondary vertices. The expected statistics are $\simeq 13\,000$ reconstructed D^0 in 10^7 central Pb–Pb events and $\simeq 20\,000$ in 10^9 pp events. The significance is larger than 10 for up to about $p_{\rm t} = 10\,{\rm GeV}/c$ both in Pb–Pb and in pp collisions. The cross-section can be measured down to $p_{\rm t} \simeq 1\,{\rm GeV}/c$ in Pb–Pb collisions and down to almost $p_{\rm t} = 0$ in pp collisions.

5. Summary

Heavy flavor production at LHC energies is a very promising tool to investigate in deep detail the characteristics of the hot and dense medium formed in heavy ion collisions and should allow to benchmark with precision pQCD calculations in pp collisions. This results from the large variety of observables which are available in the different heavy flavor channels. The excellent expected performances of the LHC detectors will allow to fully exploit this rich environment and ensure an exciting physics program with heavy flavors. Details about the LHC quarkonium physics program (not covered here) can be found in [3, 7, 8].

REFERENCES

[1] N. Armesto *et al., J. Phys. G* **35**, 054001 (2008) [arXiv:0711.0974[hep-ph]].

[2] J. Baines *et al.*, arXiv:hep-ph/0601164.

[3] [ALICE Collaboration] B. Alessandro *et al.*, *J. Phys. G* **32**, 1295 (2006).

[4] K.J. Eskola, H. Paukkunen, C.A. Salgado, arXiv:0802.0139 [hep-ph].

[5] [ALICE Collaboration] Z. Conesa del Valle, *Eur. Phys. J.* **C49**, 149 (2007) [arXiv:nucl-ex/0609027]; Z. Conesa del Valle, private communication.

[6] [ALICE Collaboration] F. Carminati *et al., J. Phys. G* **30**, 1517 (2004).

[7] D.G. d'Enterria *et al.*, *J. Phys. G* **34**, 2307 (2007).

[8] [ATLAS Collaboration], CERN/LHCC/2004–009.

[9] D. Acosta *et al.*, arXiv:hep-ex/0412071.

[10] I.P. Lokhtin, A.M. Snigirev, *Eur. Phys. J.* **C21**, 155 (2001).

[11] [UA1 Collaboration] C. Albajar *et al., Phys. Lett.* **B213**, 405 (1988); *Phys. Lett.* **B256**, 121 (1991) [Erratum **B262**, 497 (1991)].

[12] [ALICE Collaboration] L. Manceau, *Eur. Phys. J.* **C62**, 9 (2009).

[13] F. Antinori *et al.*, ALICE Collaboration internal note ALICE-INT-2006-015.

[14] A. Dainese, *Nucl. Phys.* **A783**, 417 (2007) [arXiv:nucl-ex/0609042].